DOI: 10.1002/anie.201209539

Heterogeneous Catalysis

In Situ Study of Catalytic Processes: Neutron Diffraction of a Methanol Synthesis Catalyst at Industrially Relevant Pressure**

Timur Kandemir, Frank Girgsdies, Thomas C. Hansen, Klaus-Dieter Liss, Igor Kasatkin, Edward L. Kunkes, Gregor Wowsnick, Nikolas Jacobsen, Robert Schlögl, and Malte Behrens*

Heterogeneous catalysts are dynamic materials that interact with substances in the gas phase that are present in catalytic reactions. Changes that may occur when a catalyst is in contact with reactive molecules comprise adsorbate-induced surface reconstruction,[1] surface segregation,[2] inclusion of foreign atoms from the gas phase into the sub-surface,[3] and compound formation in the bulk, such as formation of oxides,[4] hydrides,[3] carbides,[5] or nitrides[6] of a metal catalyst. These modifications will affect the catalytic properties and depend on the chemical potential of the gas-phase species. An extrapolation of experimental results obtained at low pressure to pressure regimes of industrial relevance is often not straightforward (the "pressure gap").[7] To better understand the impact of dynamic catalyst changes, application of in situ techniques[8] working at industrially relevant conditions is desirable. Herein, we report on the potential of neutron diffraction (ND) as a method for in situ analysis of heterogeneous catalysts. ND studies have been carried out on many inorganic materials in various sample environments.[9] Pioneering in situ ND studies of catalysts has been performed by Turner et al.[10] and Walton et al.[11] Inelastic neutron scattering was used for catalyst characterization, for example by the groups of Albers, Lennon, and Parker.[12]

Similar to in situ XRD,[13] ND is complementary to other in situ techniques used in catalysis research, such as ambient pressure XPS,[14] XAFS,[15] or Raman spectroscopy.[16] It is uniquely suitable for in situ studies in thick-walled metallic tubular reactors, which allow application of realistic reaction conditions. No special pressure-tight windows or complex reactor design is required if a wall material is chosen that shows only minor absorption of neutrons and thus allows sufficient penetration through the walls.[17] ND is a bulk-sensitive method that gives quantitative, average structural (lattice parameter), and microstructural (domain size, lattice strain, defects) information. In contrast to XRD, the scattering power is independent of the diffraction angle providing diffraction peaks at higher angles with higher intensity. This is in particular useful for the investigation of nanomaterials with highly symmetric crystal structures that often suffer from few and weak XRD peaks available for structural analysis. Figure 1 compares ex situ ND with XRD data and shows a TEM image of the $Cu/ZnO/Al_2O_3$ catalyst used in this study.

Such catalysts are employed for the industrial synthesis of methanol from syngas ($H_2/CO/CO_2$). While being used today mainly as a base chemical and a feedstock for chemical industry, methanol has interesting potential as a sustainable synthetic fuel in a future energy scenario[18] if produced from anthropogenic CO_2 and regenerative H_2. The exothermic methanol formation is favored at low temperatures and high pressures. In the industrial process it is conducted at $T = 493$–573 K and $P = 3.5$–10 MPa.[19]

The nature of the active sites of $Cu/ZnO/Al_2O_3$ catalysts and of the often observed "Cu–ZnO synergy" has been actively debated.[19b] For instance, a model emphasizing the role of defects found in the active Cu phase after the industrially applied synthesis[20] seems in apparent contradiction to a model focusing on the dynamic interaction of Cu and ZnO leading to dynamic morphology changes of the Cu particles.[21] The latter was related to metal–support interactions and observed on supported model catalysts. Owing to the high mobility of Cu according to this model, annealing of structural defects can be expected under working conditions. Based on a structure–activity correlation and DFT calculations, we have recently presented a model for the active site of methanol synthesis that combines both views.[22] Planar defects have been shown to lead to changes in surface faceting of the Cu nanoparticles associated with formation of steps and kinks that represent high-energy surface sites of special catalytic activity. For a series of Cu/ZnO-based catalysts, a linear correlation of the defect concentration with the intrinsic activity of the exposed Cu surface was observed. Furthermore, surface decoration[21a] of Cu with ZnO_x by a strong metal–support interaction[23] (SMSI) has been confirmed by HRTEM and in situ XPS on a high-performance catalyst.[22]

---

[*] T. Kandemir, Dr. F. Girgsdies, Dr. I. Kasatkin, Dr. E. L. Kunkes, G. Wowsnick, Prof. Dr. R. Schlögl, Dr. M. Behrens
Fritz-Haber-Institut der Max-Planck-Gesellschaft
Department of Inorganic Chemistry
Faradayweg 4–6, 14195 Berlin (Germany)
E-mail: behrens@fhi-berlin.mpg.de

Dr. T. C. Hansen
Diffraction Group, Institut Laue-Langevin
38042 Grenoble (France)

Dr. K.-D. Liss
The Bragg Institute
Australian Nuclear Science and Technology Organisation
Lucas Heights, NSW 2234 (Australia)

Dr. N. Jacobsen
Clariant Produkte (Deutschland) GmbH, BU Catalysts
(formerly Süd-Chemie), 83052 Bruckmühl (Germany)

[**] The authors would like to thank M. Tovar, A. Daramsy, S. Olsen, and E. Stotz for technical support. Financial support was given by the DFG (BE 4767/1-1) and by the Bayerisches Wissenschaftsministerium (NW-0810-0002). ILL and ANSTO are acknowledged for the allocation of beamtime.

Supporting information for this article is available on the WWW under http://dx.doi.org/10.1002/anie.201209539.

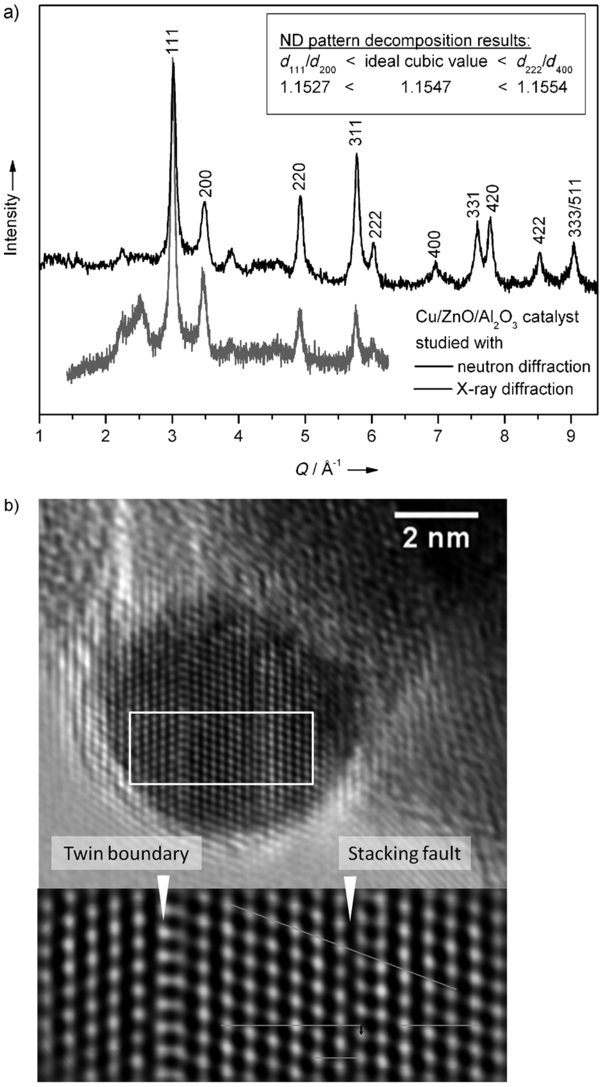

Figure 1. a) Diffraction pattern of the freshly reduced Cu/Zn/Al$_2$O$_3$ catalyst acquired at room temperature with ND (black pattern) and laboratory XRD (Cu$_{K\alpha}$, gray pattern). Peaks that are due to Cu are indexed. Owing to different wavelengths used, the abscissa is given in reciprocal space. b) High-resolution TEM image of a typical ellipsoidal copper particle in the catalyst. Planar defects and the resulting thin hcp domain are marked in the close-up.

Therefore, ZnO rather than Cu seems to be the mobile component in course of Cu–ZnO interaction, thus enabling dynamic changes and a static Cu defect structure at the same time. The predominating planar defects in the Cu particles are twin boundaries and stacking faults that can be observed in TEM images (Figure 1b) and quantitatively studied with diffraction techniques.

In the present study, an industrial Cu/ZnO/Al$_2$O$_3$ catalyst with similar properties as the materials presented in reference [20] has been used for methanol synthesis and its microstructure has been studied near industrial working conditions using in situ ND. A typical syngas mixture was applied at 523 K and 6 MPa in a continuous flow reactor, which was described in detail elsewhere.[17] Catalytic activity studies in the laboratory at differential conditions confirmed stable methanol productivity in the range reported for state-of-the-art Cu/ZnO/Al$_2$O$_3$ catalysts. During the ND experiment the reaction was in thermodynamic equilibrium, simulating the chemical potentials of the gas phase in an industrial reactor near the very end of the catalyst bed and in the outlet. At the same time, equilibrium guarantees a largely homogeneous and gradient-free catalyst bed for ND studies. Analogous in situ diffraction studies were carried out in a high-flux experiment with a time resolution of 5 min (ILL, Grenoble, France)[24] and in an experiment with high instrumental resolution (Bragg Institute, Lucas Heights, Australia).[25] The catalyst was reduced in a D$_2$ stream in the reactor prior to the catalytic reaction. During the in situ study, methanol was detected at the outlet of the reactor by mass spectrometry. Figure 2 shows the high-resolution neutron diffraction patterns of the reduced catalyst in 0.1 MPa Ar at 523 K right before the synthesis and during synthesis under 6 MPa of syngas after 3 and 24 h time-on-stream (TOS).

The Rietveld fit of the fresh catalyst in Ar (Figure 2, top) reveals the presence of fcc-Cu as the major phase, with a unit cell length of $a = (3.6268 \pm 0.0008)$ Å at 523 K (more results of the Rietveld analysis are presented in the Supporting Information). Additional weaker peaks of the catalyst are due to the ZnO component (Figure 2, green profile). No major changes of the Cu phase are obvious from a first comparison of the three ND patterns recorded at different conditions, and the lattice parameter of Cu does not vary significantly. Thus, bulk inclusion of C or H species from the gas phase in the Cu lattice of working catalysts can be readily excluded. Only a slight sharpening of the Cu peaks can be detected, which corresponds to an increase in crystalline domain size from (5.9 ± 0.1) nm to (6.4 ± 0.1) nm with time and is due to sintering of the Cu particles, which is a relevant deactivation mechanism of methanol synthesis catalysts.[26]

Planar defects have been observed in a comparative TEM and XRD study of similar Cu/ZnO/Al$_2$O$_3$ catalysts.[20] Such defects are expected to contribute to the anisotropic broadening of the ND peaks, but line profile analysis turned out to be complex and data analysis suffered from the nanostructured nature of the samples and the in situ conditions (for details, see the Supporting Information). However, application of a pattern decomposition method has been shown[22] to allow qualitative confirmation of the presence of stacking faults in the Cu nanoparticles. This evaluation is based on the peak positions, which can be determined with higher precision compared to the other peak profile parameters.

An ideal defect-free Cu is expected to show a ratio of the distances between the (111) and (200) lattice planes of $2/\sqrt{3} = 1.1547$. The presence of stacking faults causes a shift of the 111 and 200 peaks towards each other and lowers this ratio.[27] Careful evaluation of the peak positions of the ex situ ND data shown in Figure 1a revealed that such a shift is also found for the catalyst under study herein. Furthermore, a consistent opposite shift of the 222 and 400 reflection pair was also observed (Figure 1a, inset), which also confirms the presence of stacking faults. Furthermore, HRTEM observations provide further evidence for this type of planar defects in the catalyst as shown in Figure 1b. The resulting deviation from cubic symmetry can be used as a measure for the

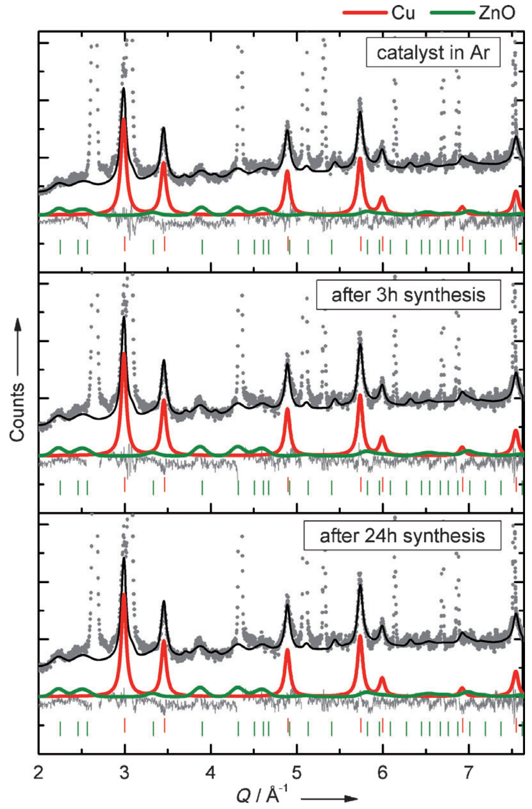

Figure 2. Rietveld fits of the catalyst before (0.1 MPa Ar, upper panel), at the beginning (center) and after 24 h of methanol synthesis (bottom) at 523 K and 6 MPa. Experimental data is shown in gray, and the calculated pattern of the catalyst as a black line. The thin gray line is the difference between experimental and calculated pattern. The contribution of the Cu phase and ZnO is marked as red and green lines with tick marks at the positions of Bragg reflections. Additional strong peaks from the Al reactor wall were treated as peak-phase during Rietveld analysis and are excluded from the overall calculated profile shown here.

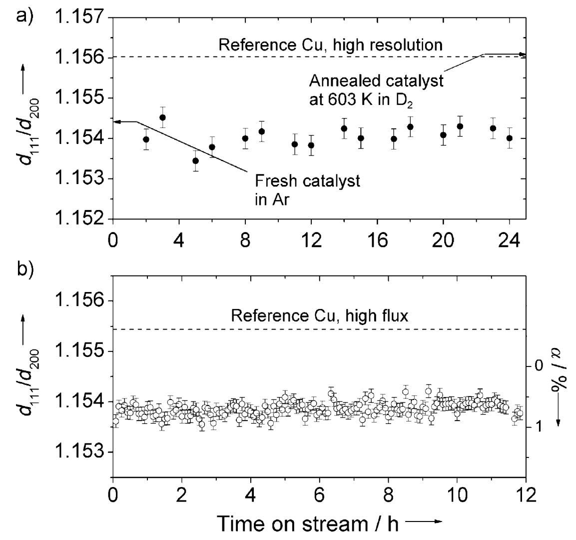

Figure 3. The d_{111}/d_{200} ratio of Cu in the catalyst and reference sample over TOS during methanol synthesis under industrially relevant conditions in the high-resolution (a) and high-flux experiments (b). This ratio is a measure for the defectiveness of Cu (see text). The formally resulting stacking fault concentration α is shown on the right axis of (b). The error bars are the standard deviations of the two datasets neglecting systematic errors that are due for example to wavelength and zero shift.

stacking fault probability α. Based on the lower-order reflection pair, which exhibits well-defined peaks even in the in situ ND data, α is calculated according to $\alpha = 8.3 \times [(2/\sqrt{3}) - (d_{111}/d_{200})]$.[27] Figure 3 shows the evolution of d_{111}/d_{200} of the Cu catalyst versus TOS during methanol synthesis.

Similar values are obtained in both the high-flux and the high-resolution experiments that are significantly lower than that observed for a macrocrystalline Cu reference powder measured in the same reactor tube. The experimental values of this defect-poor reference deviate from the theoretical value expected for a perfect fcc lattice in both experiment (compare right hand axis in Figure 3b). This situation is attributed to systematic displacement errors of the complex in situ cell at the beamline, which will lead to an offset-like effect in d_{111}/d_{200} and also causes the slight difference of this parameter obtained from ex situ and in situ data of the same catalyst as seen in Figure 1a and Figure 3. Thus, in contrast to previously reported ex situ ND data,[22] α is evaluated in a semi-quantitatively fashion in this study and only the consistent internal trends observed during the two in situ experiments are discussed in the following. However, the magnitude of deviation between catalyst and reference on the α scale corresponds to a few percent, which is in agreement with previous studies of similar materials.[20,22]

These results confirm that the Cu phase in the active catalyst bears stacking faults. Furthermore, this data proves that the planar defects in the Cu nanoparticles are relatively stable under working conditions and do not disappear when switching from Ar to syngas on a time scale proposed for Cu morphology changes (< 30 min[21c]), but resist for 24 h TOS. Annealing of the defects would lead to an approach toward the reference value for d_{111}/d_{200}, which is in both experiments hardly significant in the investigated time interval.

Figure 3 reveals that the difference between the catalytically active copper phase and a bulk reference copper material, which has been observed before[20] and ascribed to the peculiar microstructure of the former,[28] is mostly conserved under working conditions. This finding supports the concept of a rather static Cu bulk phase, which maintains its defect structure. No conclusion about dynamic surface behavior, such as surface diffusion, surface reconstruction, or re-crystallization, can be made based on these results obtained by a bulk diffraction method. Such surface mobility (and an effect of the gas atmosphere on it) seems to be even very likely considering the low Hüttig temperature of Cu and the beginning sintering of the nanoparticles observed in the experiment.

However, the bulk stability of the Cu particles suggest that the observed strong interactions between Cu and ZnO[22] manifest themselves rather in form of mobile ZnO_x than mobile Cu in the industrial high performance catalyst. The material under study herein exhibits relatively large Cu nanoparticles and poorly crystalline ZnO, and the observations are not necessarily in contradiction with previous reports of a mobile Cu phase and static ZnO, which were made on highly crystalline ZnO decorated with very small Cu particles,[21] as such differences might be able to cause to a switch of the mobile component during SMSI-induced dynamics.

To study the response of the catalyst to higher T than applied for methanol synthesis, the sample was heated after the 24 h TOS experiment in a D_2 atmosphere to 603 K (high-resolution experiment) and 653 K (high-flux experiment). This is beyond the temperature limit of approximately 573 K, which should not be exceeded in methanol synthesis to suppress activity loss owing to sintering.[26a] At 603 K the Cu crystallites have grown significantly to (9.4 ± 0.2) nm, as revealed by ND peak width analysis. At the same time, the defects have also been annealed and α is at the same level as the bulk reference (Figure 3 a), showing the strong effect of temperature on the bulk mobility of the Cu particles by approaching the Tammann temperature. According to a simple estimation, bulk re-crystallization is expected to start at 0.5 T_M, which in case of Cu is at 679 K.

The evolution of the Cu lattice parameter over the full temperature range is shown in Figure 4 (high-flux data). The thermal expansion of the reference Cu powder as well as of the catalyst is linear at $T < 523$ K. Interestingly, the lattice parameters at room temperature as well as the thermal expansion coefficient of catalyst and reference differ. The extrapolated Cu lattice parameter is (3.6114 ± 0.0009) Å for the catalysts and thus 0.1% smaller than that of the bulk reference, which corresponds to the literature value. The slightly lower value for the catalyst is in agreement with ex situ results[22] and is ascribed to the complex microstructure of the composite catalyst. Lattice contraction might be due to the lower particles size as observed for many metals[29] or to the effect of defects. However, as the metal particles in this catalyst are relatively large and the effect of stacking faults on the average lattice parameter is low, the most likely explanation is the interfacial contact with the oxide phase. Different thermal expansion coefficients have also been previously observed for nanomaterials compared to their bulk counterparts[30] and are probably also influenced by the contact to the oxide phase and the presence of defects.

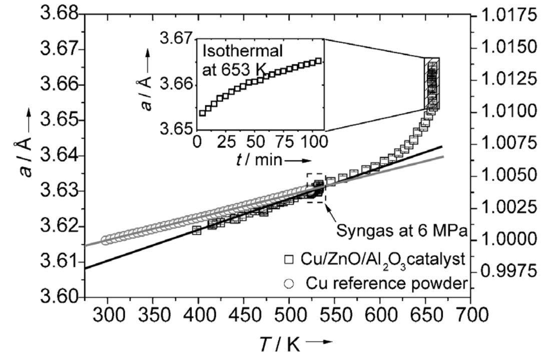

Figure 4. Evolution of the lattice parameter of Cu in the $Cu/ZnO/Al_2O_3$ catalyst and of the Cu reference powder with temperature. The Cu powder was heated in Ar at 0.1 MPa, while the calcined catalyst was heated to 523 K in D_2 (0.1 MPa), then subjected to 12 h of methanol synthesis at 523 K in the syngas feed (6 MPa), and finally heated in D_2 (0.1 MPa) to 653 K. The heating rate was 1 $K\,min^{-1}$ and one ND pattern corresponds to circa 5 K. The dashed square at 523 K marks the period of 12 h synthesis. The right axis shows the lattice expansion relative to the reference at 298 K.

The period of methanol synthesis over 12 h (dashed square in Figure 4) did not lead to any lattice expansion. Thus the beginning formation of α-brass in the bulk of the Cu particles by partial reduction of the ZnO component can be safely excluded during methanol synthesis under industrial conditions. Spencer[31] reported a low diffusion coefficient of zinc in copper at methanol synthesis condition of 523 K that increased when increasing the temperature to 623 K. Accordingly, brass formation is observed at higher temperature in D_2 and causes a deviation from the linear behavior starting at around 603 K. In this temperature regime, thermal expansion is superimposed to the lattice expansion due to successive substitution of Cu by larger Zn atoms in the newly formed alloy as is evidenced by the continuing lattice expansion in the isothermal regime at 653 K (Figure 4, inset). Based on the results of Grazzi et al.,[32] the concentration of Zn in the alloy can be estimated to be (4.88 ± 0.05) wt% after 100 min of isothermal treatment at 653 K in 0.1 MPa D_2.

In summary, the potential of in situ ND to study solid catalysts in a realistic reactor under high-pressure conditions that are relevant for applications has been demonstrated for a $Cu/ZnO/Al_2O_3$ methanol synthesis catalyst. The metallic Cu component is nanostructured and has many and different kinds of defects. The deviation from ideal bulk Cu is manifested in a lattice contraction at room temperature and an increased thermal expansion coefficient. Furthermore, a high concentration of stacking faults has been detected in the Cu nanoparticles. These bulk defects were stable upon changing the gas atmosphere to partial pressures as applied in industrial methanol synthesis. Also, the bulk inclusion of reactive species from the gas phase as well as the formation of brass during methanol synthesis can be excluded. The latter alloying as well as the annealing of the bulk defects was observed only at significantly higher temperatures than used in the industrial process. Under the reaction conditions, the bulk integrity of the nanoparticles as well as the non-ideal nature of Cu was found to be relatively stable in industrial catalysts. Thus, the results suggest that the interaction between metal and oxide during methanol synthesis involves dynamics of the poorly crystalline ZnO component rather than of the entire bulk of the Cu particles and this affects only the Cu surface. Future work using this method will aim at correlation of the described structural properties with catalytic performance and include information about the evolution of the microstructure with deactivation of the catalyst over a longer TOS.

Experimental Section

The catalyst was provided by Clariant Produkte (Deutschland) GmbH. The methanol synthesis reaction was done at 523 K and 6 MPa in thermodynamic equilibrium with a syngas mixture (CO_2/CO/D_2/Ar = 8:6:75:6) in a flow cell described previously.[17] Diffraction experiments were carried out on D1B (ILL, Grenoble, France)[24a] and on ECHIDNA (ANSTO, Lucas Heights, Australia).[25] Sieve fractions of the catalyst and the polycrystalline Cu reference (99.8%, Heraeus) were used (200–300 μm). Rietveld refinement was carried out with the Topas 4.2[33] software. Multiple peak fitting during pattern decomposition was carried out with OriginPro 8.5 (OriginLab Corporation) peak analyzer. For more experimental details, see the Supporting Information.

Received: November 28, 2012
Revised: January 5, 2013

Keywords: $Cu/ZnO/Al_2O_3$ catalyst · heterogeneous catalysis · in situ studies · methanol synthesis · neutron diffraction

---

[1] a) K. Christmann, F. Chehab, V. Penka, G. Ertl, *Surf. Sci.* **1985**, *152–153 Part 1*, 356; b) G. A. Somorjai, M. A. Van Hove, *Prog. Surf. Sci.* **1989**, *30*, 201.

[2] a) K. J. J. Mayrhofer, V. Juhart, K. Hartl, M. Hanzlik, M. Arenz, *Angew. Chem.* **2009**, *121*, 3581; *Angew. Chem. Int. Ed.* **2009**, *48*, 3529; b) P. Strasser, S. Koh, T. Anniyev, J. Greeley, K. More, C. F. Yu, Z. C. Liu, S. Kaya, D. Nordlund, H. Ogasawara, M. F. Toney, A. Nilsson, *Nat. Chem.* **2010**, *2*, 454.

[3] D. Teschner, J. Borsodi, Z. Kis, L. Szentmiklósi, Z. Révay, A. Knop-Gericke, R. Schlögl, D. Torres, P. Sautet, *J. Phys. Chem. C* **2010**, *114*, 2293.

[4] G. R. Patzke, Y. Zhou, R. Kontic, F. Conrad, *Angew. Chem.* **2011**, *123*, 852; *Angew. Chem. Int. Ed.* **2011**, *50*, 826.

[5] J. W. Niemantsverdriet, A. M. Van der Kraan, W. L. Van Dijk, H. S. Van der Baan, *J. Phys. Chem.* **1980**, *84*, 3363.

[6] B. Herzog, D. Herein, R. Schlögl, *Appl. Catal. A* **1996**, *141*, 71.

[7] a) J. A. Dumesic, G. W. Huber, M. Boudart, in *Handbook of Heterogeneous Catalysis*, Wiley-VCH, Weinheim, **2008**; b) M. Hävecker, A. Knop-Gericke, T. Schedel-Niedrig, R. Schlögl, *Angew. Chem.* **1998**, *110*, 2049; *Angew. Chem. Int. Ed.* **1998**, *37*, 1939.

[8] a) *In Situ Spectroscopy of Catalysts: X-Ray Diffraction and Scattering* (Ed.: B. Weckhuysen), Amercian Scientific Publishers, New York, **2004**; b) A. Brückner, *Catal. Rev.* **2003**, *45*, 97.

[9] I. F. Bailey, *Z. Kristallogr.* **2003**, *218*, 84.

[10] J. F. C. Turner, R. Done, J. Dreyer, W. I. F. David, C. R. A. Catlow, *Rev. Sci. Instrum.* **1999**, *70*, 2325.

[11] R. I. Walton, R. J. Francis, P. S. Halasyamani, D. O'Hare, R. I. Smith, R. Done, R. J. Humphreys, *Rev. Sci. Instrum.* **1999**, *70*, 3391.

[12] a) D. Lennon, D. T. Lundie, S. D. Jackson, G. J. Kelly, S. F. Parker, *Langmuir* **2002**, *18*, 4667; b) A. R. McInroy, D. T. Lundie, J. M. Winfield, C. C. Dudman, P. Jones, S. F. Parker, J. W. Taylor, D. Lennon, *Phys. Chem. Chem. Phys.* **2005**, *7*, 3093; c) A. R. McInroy, D. T. Lundie, J. M. Winfield, C. C. Dudman, P. Jones, S. F. Parker, D. Lennon, *Catal. Today* **2006**, *114*, 403; d) S. F. Parker, J. W. Taylor, P. Albers, M. Lopez, G. Sextl, D. Lennon, A. R. McInroy, I. W. Sutherland, *Vib. Spectrosc.* **2004**, *35*, 179; e) P. W. Albers, S. F. Parker, in *Neutron Applications in Earth, Energy, and Environmental Sciences* (Eds.: L. Liang, R. Rinaldi, H. Schober), Springer, New York, **2009**, p. 391.

[13] R. Schlögl, *Adv. Catal.* **2009**, *52*, 273.

[14] M. Salmeron, R. Schlögl, *Surf. Sci. Rep.* **2008**, *63*, 169.

[15] J. D. Grunwaldt, B. S. Clausen, *Top. Catal.* **2002**, *18*, 37.

[16] I. Wachs, *Top. Catal.* **1999**, *8*, 57.

[17] T. Kandemir, D. Wallacher, T. Hansen, K.-D. Liss, R. Naumann d'Alnoncourt, R. Schlögl, M. Behrens, *Nucl. Instrum. Methods Phys. Res. Sect. A* **2012**, *673*, 51.

[18] G. A. Olah, A. Goeppert, G. K. S. Prakash, *Beyond Oil and Gas: The Methanol Economy*, Wiley-VCH, Weinheim, **2006**.

[19] a) E. Fiedler, G. Grossmann, D. B. Kersebohm, G. Weiss, C. Witte in *Ullmann's Encylopedia of Industrial Chemistry*, Wiley-VCH, Weinheim, **2011**; b) J. B. Hansen, P. E. Højlund Nielsen in *Handbook of Heterogeneous Catalysis*, Wiley-VCH, Weinheim, **2008**.

[20] I. Kasatkin, P. Kurr, B. Kniep, A. Trunschke, R. Schlögl, *Angew. Chem.* **2007**, *119*, 7465; *Angew. Chem. Int. Ed.* **2007**, *46*, 7324.

[21] a) J. D. Grunwaldt, A. M. Molenbroek, N. Y. Topsoe, H. Topsoe, B. S. Clausen, *J. Catal.* **2000**, *194*, 452; b) P. L. Hansen, J. B. Wagner, S. Helveg, J. R. Rostrup-Nielsen, B. S. Clausen, H. Topsoe, *Science* **2002**, *295*, 2053; c) P. C. K. Vesborg, I. Chorkendorff, I. Knudsen, O. Balmes, J. Nerlov, A. M. Molenbroek, B. S. Clausen, S. Helveg, *J. Catal.* **2009**, *262*, 65.

[22] M. Behrens, F. Studt, I. Kasatkin, S. Kühl, M. Havecker, F. Abild-Pdersen, S. Zander, F. Girgsdies, P. Kurr, B. Kniep, M. Tovar, R. W. Fischer, J. K. Nørskov, R. Schlögl, *Science* **2012**, *336*, 893.

[23] R. Naumann d'Alnoncourt, X. Xia, J. Strunk, E. Loffler, O. Hinrichsen, M. Muhler, *Phys. Chem. Chem. Phys.* **2006**, *8*, 1525.

[24] a) I. P. Orench, J. A. R. Velamazán, J. Campo, *Neutron News* **2010**, *21*, 20; b) R. Allemand, J. Bourdel, E. Roudaut, P. Convert, K. Ibel, J. Jacobe, J. P. Cotton, B. Farnoux, *Nucl. Instrum. Methods* **1975**, *126*, 29.

[25] K.-D. Liss, B. Hunter, M. Hagen, T. Noakes, S. Kennedy, *Phys. B Condensed Matter* **2006**, *385–386 Part 2*, 1010.

[26] a) M. V. Twigg, M. S. Spencer, *Top. Catal.* **2003**, *22*, 191; b) G. Prieto, J. Zečević, H. Friedrich, K. P. de Jong, P. E. de Jongh, *Nat. Mater.* **2013**, *12*, 34.

[27] B. E. Warren, *Prog. Met. Phys.* **1959**, *8*, 147.

[28] M. M. Günter, T. Ressler, B. Bems, C. Buscher, T. Genger, O. Hinrichsen, M. Muhler, R. Schlögl, *Catal. Lett.* **2001**, *71*, 37.

[29] a) R. Lamber, S. Wetjen, N. I. Jaeger, *Phys. Rev. B* **1995**, *51*, 10968; b) Z. Huang, P. Thomson, S. Di, *J. Phys. Chem. Solids* **2007**, *68*, 530.

[30] a) J. Hu, W. Cai, C. Li, Y. Gan, L. Chen, *Appl. Phys. Lett.* **2005**, *86*, 151915; b) A. Plech, V. Kotaidis, S. Grésillon, C. Dahmen, G. von Plessen, *Phys. Rev. B* **2004**, *70*, 195423.

[31] M. S. Spencer, *Surf. Sci.* **1987**, *192*, 329.

[32] F. Grazzi, L. Bartoli, S. Siano, M. Zoppi, *Anal. Bioanal. Chem.* **2010**, *397*, 2501.

[33] *Topas 4.2*, Bruker AXS GmbH, **2010**; http://www.bruker-axs.de/topas.html.